Materials Physics and Mechanics 48 (2022) 124-135
Research article

Received: November 1, 2021
Accepted: March 9, 2021

EXPERIMENTAL SUBSTANTIATION OF THE POSSIBILITY OF HYDROLYTIC LIGNIN USING IN THE ARCHITECTURAL ELECTROMAGNETIC SHIELDING SYSTEMS

O.V. Boiprav[1]✉, N.N. Grinchik[2], G.A. Pukhir[3]

[1] Belarusian State University of Informatics and Radioelectronics, 6, P. Brovki Str., Minsk, 220013, Republic of Belarus

[2] A.V. Luikov Heat and Mass Transfer Institute of NAS of Belarus, 6, P. Brovki, Minsk, Republic of Belarus, 220072

[3]Educational Establishment "Belarusian State University of Informatics and Radioelectronics", 6, P. Brovki Str., 6, Minsk, Belarus

✉ smu@bsuir.by

Abstract. The article presents the research results of electromagnetic radiation reflection and transmission characteristics in the frequency range 0.7–17.0 GHz of the hydrolytic lignin, impregnated to saturation with the electrolyte water solution, at different temperatures of this material. The research is aimed at simultaneously solving of two problems: 1) search for new inexpensive materials for electromagnetic shielding; 2) experimental substantiation of a new promising method of hydrolysis lignin utilization. Based on the research results, it is possible to conclude the hydrolytic lignin is prospective for use for the manufacture of moisture-containing materials that attenuate electromagnetic radiation energy. Such materials could be used in the architectural electromagnetic shielding systems (including in the systems operating under conditions other than standard) in the form of filler for air gaps of walls and floors or filler for the building mixtures. In practice, such systems are used for protection radioelectronic equipment or people, located inside of the buildings, from the impact of external electromagnetic radiation.

Keywords: hydrolytic lignin, architectural electromagnetic shielding, electromagnetic radiation reflection and transmission coefficients, calcium chloride.

Acknowledgements. *No external funding was received for this study.*

Citation: Boiprav O.V., Grinchik N.N., Pukhir G.A. Experimental Substantiation of The Possibility of Hydrolytic Lignin Using in the Architectural Electromagnetic Shielding Systems // Materials Physics and Mechanics. 2022, V. 48. N. 1. P. 124-135. DOI: 10.18149/MPM.4812022_11.

1. Introduction

In works [1-3] the problem of the lignin utilization and processing is actualized. The problem is due to the following reasons:

1) an average of 70 million tons of lignin is produced in the world annually;

http://dx.doi.org/10.18149/MPM.4812022_11

2) industrial processing of lignin at present seems to be a difficult task, which is associated with the complex composition of this material, as well as with the instability of its chemical properties due to the dependence of the latter on the nature of the thermal effect exerted on it;
3) in dry form, lignin is a flammable, combustible and explosive material.

Lignin is a waste of the physicochemical processing of plant raw materials (mainly wood). There are several modifications of lignin, depending on the specifics of the production, during which it is formed:

1) hydrolytic (sulfur-free or powder) lignin, which is a waste product from the processing of raw materials used in the hydrolysis industry; lignin of this modification is stored in special storage facilities of the hydrolysis industry enterprise;

2) sulfate lignin, which is a waste product of the processing of raw materials used in the cellulose industry, characterized by the property of solubility in water; lignin of this modification is largely utilized in power plants of the cellulose industry;

3) sulfite lignin, as well as sulfate lignin, which is a waste product from the processing of raw materials used in the cellulose industry, characterized by the property of solubility in water; unlike sulfate lignin, lignin of the considered modification is partly stored in special storage facilities of a pulp industry enterprise, and partly goes along with wastewater from such an enterprise into rivers and/or lakes [4].

Thus, the problem of hydrolytic lignin utilization and processing is more urgent than the problem of sulfate or sulfite lignin processing.

Nowadays, the following ways of lignin utilization are known:
1) use of the lignin like the carbon source [5-7];
2) manufacturing hydrogel on the base of the lignin [8-10];
3) use of the lignin like the component of air filtering materials [11,12];
4) use of the lignin like the component of UV absorbers [13-15].

It was noted in paper [16], that new strategies of lignin use should be developed, due to the fact, that the problem of this material utilization is still unresolved. In connection with the above, the aim of the presented work was to experimentally substantiate of new approach of the hydrolytic lignin utilization. According to this approach, lignin could be used as the base for obtaining moisture-containing materials that are suitable for use in the architectural electromagnetic shielding systems (including in systems operated under conditions other than standard). In practice, such systems are used for protection radioelectronic equipment and people, located inside the buildings, from the impact of external electromagnetic radiation. The aim has been set according to the following premises:
1) hydrolytic lignin is characterized by the sorption properties [17-19];
2) moisture-containing materials are effective ones for proving electromagnetic radiation losses [20-22];
3) hydrolytic lignin (both dry and wet) is characterized by the thermal insulation properties [23].

To achieve the aim, the following tasks have been solved:
1) methods for study the electromagnetic radiation reflection coefficient (S_{11}) and electromagnetic radiation transmission coefficient (S_{21}) characteristics have been developed;
2) S_{11} and S_{21} characteristics of moisture-containing hydrolysis lignin at different temperatures have been obtained.

2. Materials and Methods

To carry out the research, the experimental sample has been made on the basis of hydrolysis moisture-containing lignin in accordance with the procedure, which includes the following stages.

Stage 1. Preparation of calcium chloride water solution of equilibrium concentration, which is 30.0 wt. %.

Stage 2. Impregnation of hydrolysis lignin until saturation with the prepared solution (the ratio of the mass of hydrolysis lignin and the maximum mass of the water solution that it can absorb and retain in the pores of its particles is 2:3).

Stage 3. Arrangement of hydrolysis lignin, impregnated to saturation with calcium chloride water solution of equilibrium concentration, in a container made of polymer heat-resistant material.

The length and width of the manufactured sample were 100 cm, its thickness was 0.5±0.1 cm.

To change the temperature of the manufactured sample (decrease from 25°C to 0°C and –20°C) during the measurement of its S_{11} and S_{21} values, as well as the temperature of the hydrolysis lignin, impregnated to saturation with calcium chloride water solution of equilibrium concentration, used for its manufacturing climatic test chamber "Mini Sabzero MS-71" has been used. The indicated limits were chosen on the basis that calcium chloride water solution of equilibrium concentration crystallizes at a temperature of ~ –20.0°C [24], and the process of water evaporation from it begins at a temperature of 25.0°C.

Figure 1 demonstrates the dynamics of changes in the temperature of the manufactured experimental sample in the range from –20°C to 70°C under standard conditions [25].

A MobIR M4 thermal imaging camera has been used to record the temperature of the manufactured experimental sample. The specified device is characterized by the measured temperatures range from –25°C to +250°C and the temperature measurement accuracy of ±2°C.

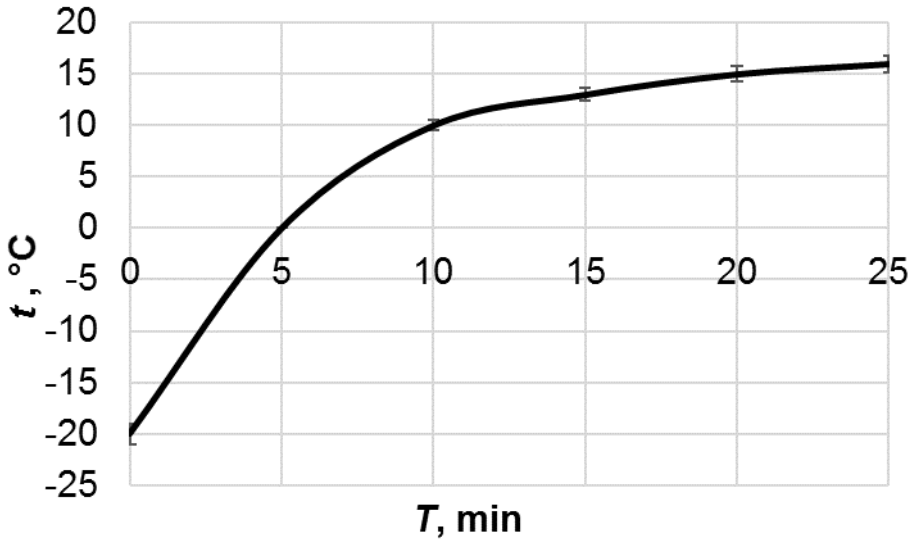

Fig. 1. Temperature dynamics of the manufactured sample

Figure 1 shows that the mathematical model of the changing process of the temperature (t) within the range of –20°C to 25°C with time (T) of the manufactured experimental sample can be approximated by a set of linear and logarithmic functions and, taking into account the accuracy of the measurements, is represented by the following expressions:

$$t = \begin{cases} 4.0 \cdot T - 20.0, \text{ if } T \in [0; 5]; \\ 10.0 \cdot \lg T + 2.0, \text{ if } T \in (5; 16]. \end{cases}$$

Measurements of S_{11} and S_{21} values of the manufactured sample have been carried out in the frequency range 0.7–17 GHz. In this case, the certified measuring system has been used. It consists of the following devices:

- the sweeping frequency generator (SFG) and the measurement signal processing unit (panoramic meter of transmission and reflection coefficients SNA 0.01-18);

- transmitting and receiving broadband horn lens antennas (operation frequency range is 0.7–17,44 GHz; the aperture size is 351×265 mm^2);
- blocks of directional couplers (blocks B and A/R) to isolate and detect electromagnetic waves incident, reflected and transmitted through the sample.

To set the measurement parameters (frequency range, type of measured value) and systematize their results, special software has been used. The measurement process included the following stages.

Stage 1. Calibration of the measuring system before measuring of S_{11} values of the manufactured sample. The calibration allowed to establish the optimal level of electromagnetic radiation power for the operation of its detectors. Figure 2 shows the connection scheme of the measuring system devices when calibration before measuring of S_{11} values. It is necessary to note, that short circuit should be used during such calibration. This element is indicated like "SC" in Fig. 2.

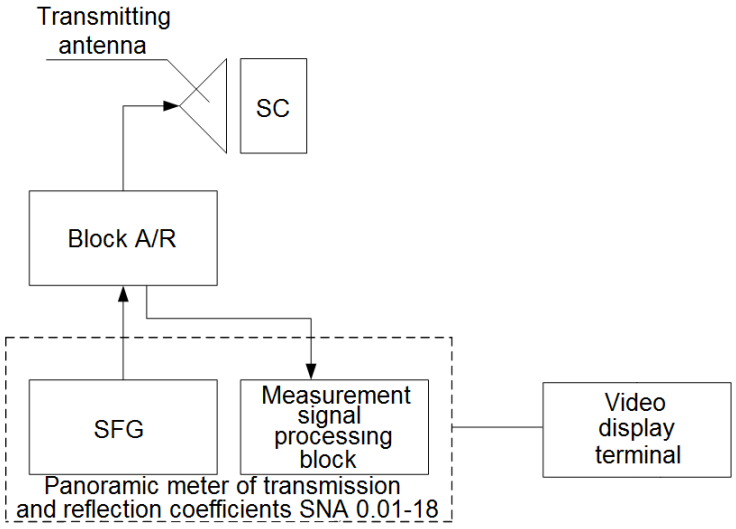

Fig. 2. The connection scheme of the measuring system devices when calibration before measuring of S_{11} values

The metal plate was used like short circuit when calibration before measuring of S_{11} values of the manufactured sample. The distance between the plate and transmitting antenna was equal to the thickness of the manufactured sample (0.5±0.1 cm). The appearance of the measuring system when calibration before measuring of S_{11} values is presented in Fig. 3.

Fig. 3. The appearance of the measuring system when calibration before measuring of S_{11} values

Stage 2. Measurement of S_{11} values of the manufactured sample. The measurement has been implemented in short circuit mode, when the manufactured sample was located between

the measurement antenna and metal plate. On the base of the measurement results obtained in such mode, it is possible to estimate the properties of the sample to absorb the electromagnetic radiation.

Figure 4 shows the connection scheme of the measuring system devices when measuring of S_{11} values.

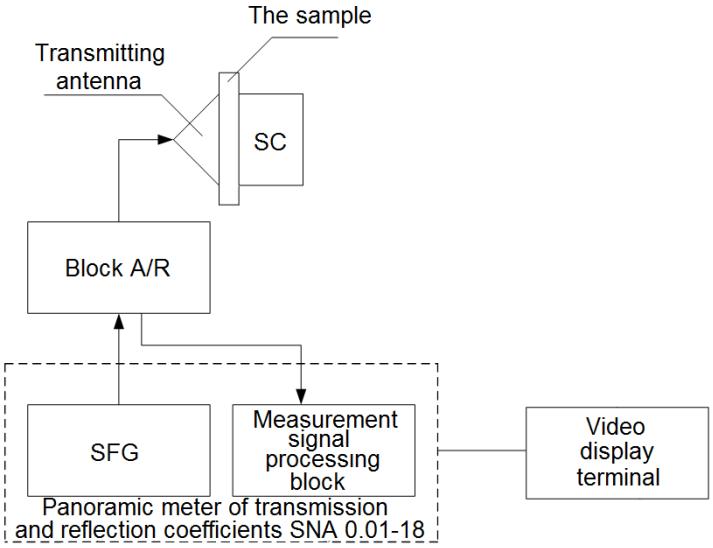

Fig. 4. The connection scheme of the measuring system devices when measuring of S_{11} values of the manufactured sample

In the course of measuring of S_{11} values, the SFG formed a signal, which was fed through the block A/R to the transmitting antenna. The measurement signal processing block was used to record the amplitude of the electromagnetic radiation reflected from the surface of the manufactured sample.

Stage 3. Calibration of the measuring system before measuring of S_{21} values of the manufactured sample. The transmitting and receiving antennas were located opposite each other during the calibration. The distance between the antennas was equal to the thickness of the manufactured sample (0.5±0.1 cm). Figure 5 shows the connection scheme of the measuring system devices when calibration before measuring of S_{21} values.

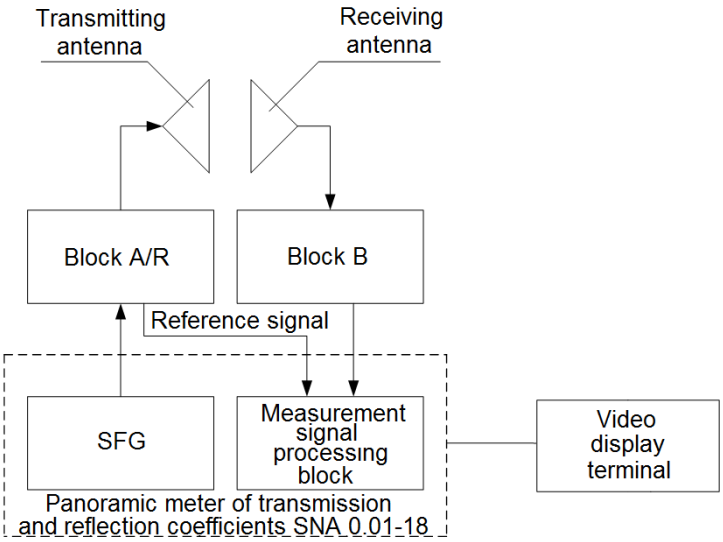

Fig. 5. The connection scheme of the measuring system devices when measuring of S_{21} values of the manufactured sample

The appearance of the measuring system when calibration before measuring of S_{21} values is presented in Fig. 6.

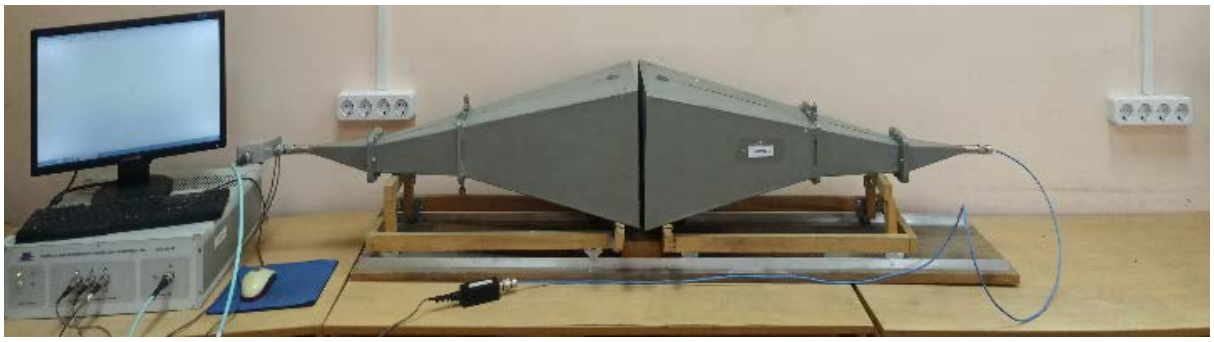

Fig. 6. The appearance of the measuring system when calibration before measuring of S_{21} values

Stage 4. Measurement of S_{21} values of the manufactured sample. In this case, the SFG formed a signal that was fed through the block A/R to the transmitting antenna. The measurement signal processing block was used to record the amplitude of electromagnetic radiation that passed through the sample under study (Fig. 7).

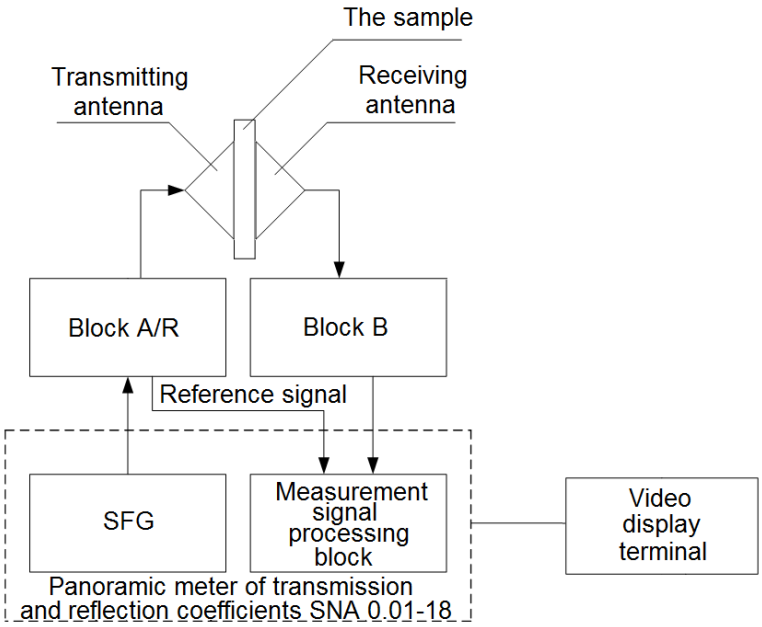

Fig. 7. The connection scheme of the measuring system devices when measuring of electromagnetic radiation transmission coefficient values of the manufactured sample

According to the technical characteristics of the used measuring system, the modulus of measuring error S_{11} and S_{21} values, provided by this system, does not exceed 10 %.

3. Results and Their Discussion

Figure 8 shows S_{11} frequency dependences in the range of 0.7–17.0 GHz of the manufactured experimental sample at different values of its temperature. These dependences demonstrate the property of the sample to absorb the electromagnetic radiation. This is due to the fact that the dependences have been obtained on the base of the results of S_{11} values measurement,

conducted under the conditions, when the sample was located between the measurement antenna and metal plate.

It follows from Fig. 8 that if the temperature of the sample is 0.0°C, then its S_{11} values in the frequency range 0.7–2.0 GHz varies within the range from –1.0 to –4.0 dB, and in the frequency range 2.0–17.0 GHz – from –3.0 to –12.0 dB. Lower S_{11} values in the frequency range 2.0–17.0 GHz of the sample compared to the similar parameter values in the frequency range 0.7–2.0 GHz are associated with the fact that with an increase in electromagnetic radiation frequency of, the share of its energy absorbed by the material with which it interacts increases. It is necessary to note, that manufactured sample provides the absorption of electromagnetic radiation in the frequency range 9.0–12.0 GHz, due to the fact that they characterized by S_{11} values less than –10.0 dB.

A decrease in the sample temperature from 0.0°C to –20°C leads to the following changes of its S_{11} values in the following frequency ranges:

1) an increase on 1.0–2.0 dB in the frequency range 0.7–1.1 GHz, on 1.0–5.0 dB in the frequency ranges 1 1.0–12.0 GHz and 13.0–17,0 GHz;
2) reduction by 1.0–5.0 dB in the frequency range 1.1–2.0 GHz, by 1.0–10.0 dB in the frequency range 6.0–11.0 GHz, by 3.0 dB at a frequency of 12.5 GHz.

S_{11} values in the frequency range 2.0–6.0 GHz of the sample remain practically unchanged when its temperature decreases from 0.0°C to –20.0°C.

An increase from 0.0°C to 25.0°C of the sample temperature leads to the following changes of its S_{11} values in the following frequency ranges:

1) reduction by 1.0–13.0 dB in the frequency ranges 6.0–8.5 GHz and 9.5–17.0 GHz;
2) an increase of 5.0 dB at a frequency of 9.0 GHz.

S_{11} values in the frequency range 0.7–6.0 GHz of the sample remain practically unchanged with an increase of its temperature from 0.0°C to 25.0°C.

In general, based on Fig. 8, it can be summarized that S_{11} characteristic in the frequency range 0.7–2.0 GHz of the manufactured experimental sample changes to a greater extent in the case of a decrease from 0.0°C to –20.0°C rather than an increase from 0.0°C to 25.0°C of its temperature, and in the frequency range 2.0–17.0 GHz – on the contrary, in the case of an increase from 0.0°C to 25.0°C, rather than decrease from 25.0°C to –20.0°C of its temperature. S_{11} values in the frequency range 0.7–1.1 GHz of the manufactured experimental sample at its temperature of –20.0°C are higher than the analogous values corresponding to its temperatures of 0.0°C and 25.0°C; in the frequency range 1.1–2.0 GHz, the opposite relationship is observed. This may be due to the fact that the mechanisms of electromagnetic radiation interaction with the manufactured experimental sample at a frequency of less than 1.1 GHz are not affected by the presence of moisture in its composition, which determines the value of its relative permittivity and, as a consequence, wave resistance. The mechanisms of electromagnetic radiation interaction with the water in the gigahertz frequency range are described in detail in [26].

Establishing the regularity of changes of S_{11} characteristics in the frequency range 2.0–17.0 GHz of the manufactured experimental sample, depending on its temperature, is not possible. This may be due to the fact that such characteristic depends not only on the temperature of the manufactured experimental sample, but also in aggregate on a number of other factors: the relative dielectric constant of hydrolytic lignin impregnated to saturation with calcium chloride water solution, the size of the hydrolytic lignin particles and their ratio with the length of electromagnetic waves of the frequency range 2.0–17.0 GHz interacting with them, the distribution of particles over the volume of the manufactured experimental sample, the distribution of calcium chloride water solution in the pores of the particles of hydrolytic lignin and in the space between these particles. In this regard, the calculation of the average S_{11} values in the frequency range 2.0–17.0 GHz has been performed. Based on the results of the

performed calculation, it was found that if the temperature of the manufactured experimental sample is –20.0°C, then its average S_{11} value in the frequency range 2.0–17.0 GHz is –6.7 dB. At temperatures of the manufactured experimental sample of 0.0°C and 25.0°C, its S_{11} values in the frequency range 2.0–17.0 GHz are –6.3 dB and –9.5 dB respectively. Thus, we can conclude that an increase from –20.0°C to 0.0°C of the temperature of the manufactured experimental sample does not significantly affect its S_{11} average value in the frequency range 2.0–17.0 GHz. An increase from 0.0°C to 25.0°C of the temperature of this sample leads to a decrease of its S_{11} average value in the frequency range 2.0–17.0 GHz, which may be associated with a decrease of its wave impedance due to a decrease of its dielectric constant due to the water evaporation from it at a temperature of 25.0°C.

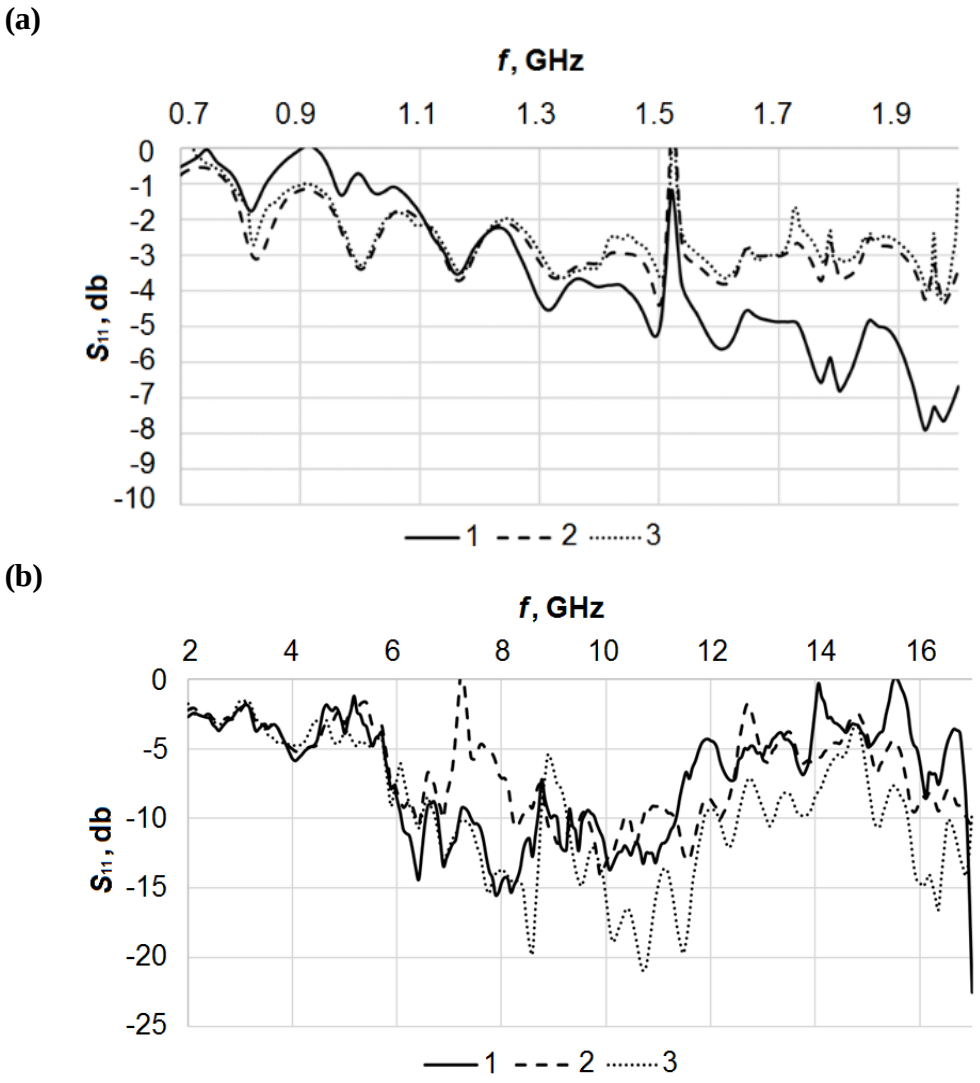

Fig. 8. S_{11} frequency dependences in the range of 0.7–2.0 GHz (a) and 2.0–17.0 GHz (b) of the manufactured experimental sample at different values of its temperature: –20.0°C (curves 1), 0.0°C (curves 2), 25.0°C (curves 3)

Figure 9 shows S_{21} frequency dependences in the range 0.7–17.0 GHz of the manufactured sample at different values of its temperature.

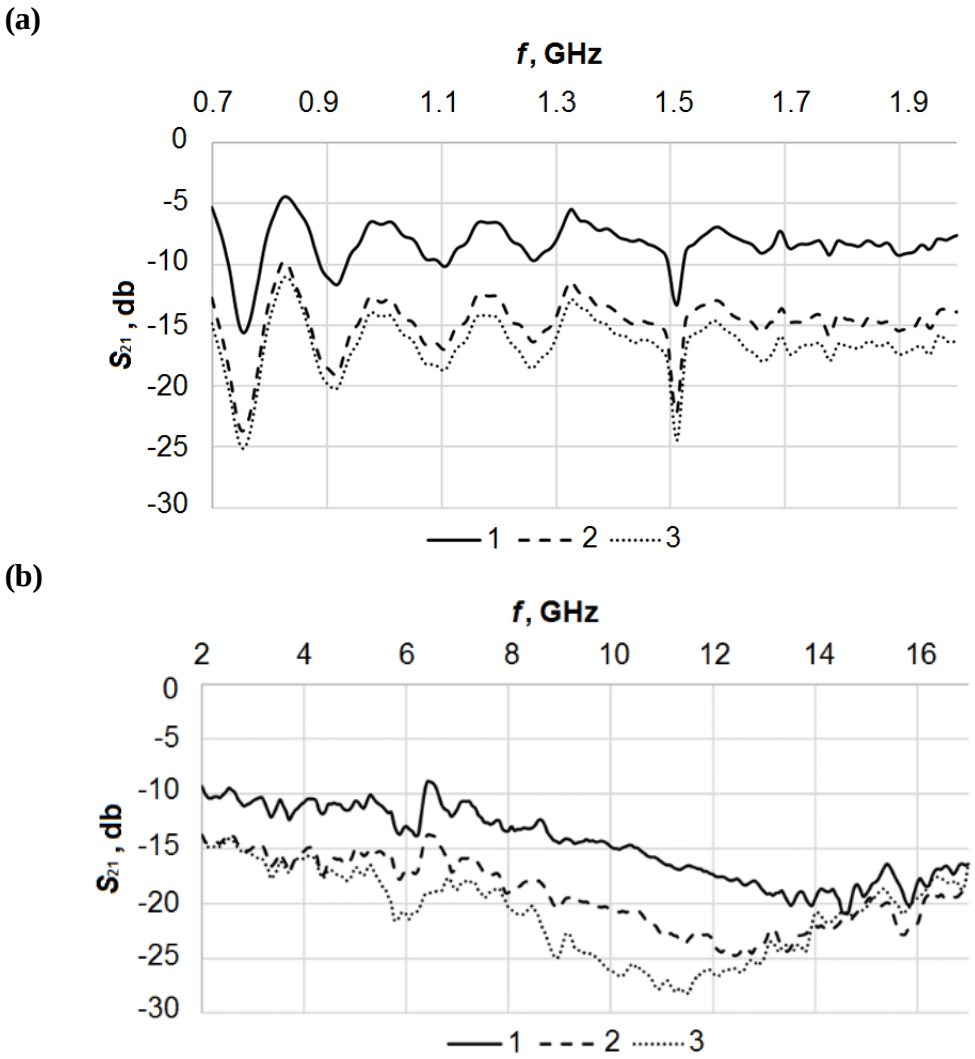

Fig. 9. S_{21} frequency dependences in the range of 0.7–2.0 GHz (a) and 2.0–17.0 GHz (b) of the manufactured experimental sample at different values of its temperature: –20.0°C (curves 1), 0.0°C (curves 2), 25.0°C (curves 3)

It follows from Fig. 9 that if the sample temperature is 25°C, then its S_{21} values in the frequency range 0.7–2.0 GHz vary within the range from –12.0 to –25.0 dB, and in the frequency range 2.0–17.0 GHz – from –15.0 to –25.0 dB. A decrease from 25°C to –20°C of the sample temperature leads to an increase of 5.0 dB in its S_{21} values in the frequency range 0.7–14.0 GHz and of 3.0 dB in the frequency range 14.0–17.0 GHz. An increase from 0.0°C to 25°C of the sample temperature leads to decrease of 1.0–5.0 dB of its S_{21} values in the frequency range 0.7–14.0 GHz and an increase of 1.0–3.0 dB of the considered parameter values in the frequency range 14.0–17.0 GHz. In general, based on Fig. 9, it can be summarized that the decrease from 25.0°C to 0.0°C and from 0.0°C to –20.0°C of the temperature of the investigated experimental sample leads to an increase of its S_{21} value in the frequency range 0.7–14.0 GHz. It could be connected with the increase of specific electrical conductivity of the hydrolysis lignin included in its composition, impregnated to saturation with calcium chloride water solution, with changes within the specified temperature limits of this material, and, as a consequence, a decrease of electromagnetic radiation energy level absorbed by them.

4. Conclusion

According to the obtained and presented results, we can to conclude, that moisture-containing hydrolytic lignin (in privacy, lignin, impregnated until saturation with the water solution of calcium chloride) are prospective for use in the architectural electromagnetic shielding systems due to its following properties:

1) S_{21} in the frequency range 0.7–17.0 GHz of this material are comparable with S_{21} of other porous materials (perlite, hydrogel, wood) [27–30]; in privacy, the material decreases in 10–300 times the energy of electromagnetic radiation in specified frequency range;

2) the shielding performance of this material does not degrade significantly if it is used at temperatures around 0 (compared with the shielding performance of this material used under the standard temperature [25]).

The studied material can be used in architectural electromagnetic shielding systems in one of the following ways:

1) like filler for air gaps of walls and floors of the buildings, where electromagnetic radiation equipment or people sensitive to the electromagnetic radiation impact are located;

2) like the filler of composite building mixture on the base of cement or gypsum for covering of the walls and floors of the buildings, specified in the previous point (also such mixture could be used for manufacturing of the panels for covering of the walls and floors of these buildings).

Thus, the aim of the presented work has been achieved.

References

[1] Chio C, Sain M, Qin W. Lignin utilization: A review of Lignin Depolymerization From Various Aspects. *Renewable and Sustainable Energy Reviews.* 2019;107: 232-249.

[2] Kumar A, Kumar J, Bhaskar T. Utilization of Lignin: A Sustainable and Eco-Friendly Approach. *Journal of the Energy Institute*. 2019;93(1): 235-271.

[3] Henriksson G, Li J, Zhang L, Lindström ME. Lignin Utilization. *RSC Energy and Environment Series*. 2010;1: 222-262.

[4] Ten E, Vermerris W. Recent Developments in Polymers Derived from Industrial Lignin. *Journal of Applied Polymer Science*. 2015;132: 42069.

[5] Rosas JM, Berenguer R, Valero-Romero MJ, Rodríguez-Mirasol J, Cordero T. Preparation of Different Carbon Materials by Thermochemical Conversion of Lignin. *Frontiers in Materials*. 2014;1: 29.

[6] Chatterjee S, Saito T. Lignin-Derived Advanced Carbon Materials. *Chemsuschem*. 2015;8(23): 3941-3958.

[7] Han J, Jeong SY, Lee JH, Choi JW, Lee JW, Roh KC. Structural and Electrochemical Characteristics of Activated Carbon Derived from Lignin-Rich Residue. *ACS Sustainable Chemistry Engineering.* 2018;7(2): 2471-2482.

[8] Larrañeta E, Imízcoz M, Toh JX, Irwin NJ, Ripolin A, Perminova A, Domínguez-Robles J, Rodríguez A, Donnelly RF. Synthesis and Characterization of Lignin Hydrogels for Potential Applications as Drug Eluting Antimicrobial Coatings for Medical Materials. *ACS Sustainable Chemistry & Engineering*. 2018;6(7): 9037-9046.

[9] Berglund L, Forsberg F, Jonoobi M, Oksman K. Promoted Hydrogel Formation of Lignin-Containing Arabinoxylan Aerogel Using Cellulose Nanofibers as a Functional Biomaterial. *RSC Advances*. 2018;8: 38219-38228.

[10] Rico-García D, Ruiz-Rubio L, Pérez-Alvarez L, Hernández-Olmos SL, Guerrero-Ramírez GL, Vilas-Vilela JL. Lignin-Based Hydrogels: Synthesis and Applications. *Polymers*. 2020;12(1): 81.

[11] Chang CY, Chang FC. Development of Electrospun Lignin-Based Fibrous Materials for Filtration Applications. *BioResourcers.* 2016;11(1): 2202-2213.

[12] Zeng Z, Ma XYD, Zhang Y, Wang Y, Ng BF, Wan MP, Lu X. Robust Lignin-Based Aerogel Filters: High-Efficiency Capture of Ultrafine Airborne Particulates and the Mechanism. *ACS Sustainable Chemistry & Engineering*. 2019;7(7): 6959-6968.
[13] Sadeghifar H, Ragauskas A. Lignin as a UV Light Blocker – A Review. *Polymers*. 2020;12(5): 1134.
[14] Zhang Y, Naebe M. Lignin: A Review on Structure, Properties, and Applications as a Light-Colored UV Absorber. *ACS Sustainable Chemistry & Engineering*. 2021;9(4): 1427-1442.
[15] Mikame K, Ohashi Y, Naito Y, Nishimura H, Katahira M, Sugawara S, Koike K, Watanabe T. Natural Organic Ultraviolet Absorbers from Lignin. *ACS Sustainable Chemistry & Engineering*. 2021;9(49): 16651-16658.
[16] Yoo CG, Ragauskas AJ. Opportunities and Challenges of Lignin Utilization. *In book: Lignin Utilization Strategies: From Processing to Applications*. Washington, DC: American Chemical Society; 2021.
[17] Hatakeyama H, Kato N, Nanbo T, Hatakeyama T. Water Absorbent Polyurethane Composites Derived from Molasses and Lignin Filled with Microcrystalline Cellulose. *Journal of Materials Science*. 2012;47(20): 7254-7261.
[18] Azhar N, Soloi S, Majid RA, Jamaluddin J. Grafting Efficiency of Lignin-Grafted-Polyacrylic Acid. *Applied Mechanics and Materials*. 2015;735: 182-185.
[19] Ma Y, Sun Y, Fu Y, Fang G, Yan X, Guo Z. Swelling behaviors of porous lignin based poly (acrylic acid). *Chemosphere*. 2016;163: 610-619.
[20] Kovaltchouk NV, Nasonova NV, Mouhamed AA, Poznyak AA. Shielding Effectiveness of Single- and Double-Layered Liquid-Containing Flexible Shields Based on Textile Materials with Gel-Powder Fillers. In: *Proceedings of the 20th International Crimean Conference Microwave & Telecommunication Technology*. 2010: 948-949.
[21] Palanisamy S, Tunakova V, Militky J, Wiener J. Effect of Moisture Content on the Electromagnetic Shielding Ability of Non‐Conductive Textile Structures. *Scientifc Reports*. 2021;11: 11032.
[22] Glyva V, Bakharev V, Kasatkina N, Levchenko O, Levchenko L, Burdeina N, Guzii S, Panova O, Tykhenko O, Biruk Y. Design of Liquid Composite Materials for Screening Electromagnetic Fields. *Eastern-European Journal of Enterprise Technologies*. 2021;6 (111): 25-31.
[23] Koptyaev VV. *Utilization of Hydrolytic Lignin During the Construction of Shallow Foundations and Earthworks. PhD Thesis.* 1999.
[24] Aïtcm P-C. Accelerators. In: *Science and Technology of Concrete Admixtures*. Elsevier; 2016. p.405-413.
[25] McNaught AD, Wilkinson A. *IUPAC. Compendium of Chemical Terminology.* Oxford: Blackwell Scientific Publications; 1997.
[26] Bhaskar T, Pandey A, Mohan SV, Lee DJ, Khanal SK. *Waste Biorefinery, Potential and Perspectives*. Elseiver; 2018.
[27] Boiprav OV, Borbotko TV, Gan'kov LL. Electromagnetic Radiation Shields With Geometrically Inhomogeneous Surface Based on Powdered Perlite and Titanomagnetite. In: *Proceedings of the 24th International Crimean Conference Microwave & Telecommunication Technology*. Sevastopol; 2014. p.639-640.
[28] Xie S, Ji Z, Yang Y, Hou G, Wang J. Electromagnetic Wave Absorption Enhancement of Carbon Black/Gypsum Based Composites Filled with Expanded Perlite. *Composites Part B: Engineering*. 2016;106: 10-19.
[29] Peymanfar R, Selseleh-Zakerin E, Ahmadi A, Saeidi A, Tavassoli SH. Preparation of Self-Healing Hydrogel Toward Improving Electromagnetic Interference Shielding and Energy Efficiency. *Scientific Reports*. 2021;11: 16161.

[30] Zhou M, Gu W, Wang G, Zheng J, Pei C, Fan F, Ji G. Sustainable Wood-Based Composites for Microwave Absorption and Electromagnetic Interference Shielding. *Journal of Materials Chemistry A*. 2020;8: 24267-24283.

THE AUTHORS

Boiprav O.V.
e-mail: smu@bsuir.by
ORCID: 0000-0002-9987-8109

Grinchik N.N.
e-mail: nngrin@yandex.by
ORCID: 0000-0002-1369-4983

Pukhir G.A.
e-mail: pukhir@tut.by
ORCID: 0000-0001-5380-8984